OATAO
Open Archive Toulouse Archive Ouverte

Open Archive Toulouse Archive Ouverte (OATAO)

OATAO is an open access repository that collects the work of Toulouse researchers and makes it freely available over the web where possible.

Attenuation of the wake of a sphere in an intense incident turbulence with large length scales

Zouhir Amoura,[1] Véronique Roig,[1] Frédéric Risso,[1] and Anne-Marie Billet[2]

[1]*Institut de Mécanique des Fluides de Toulouse (IMFT), Université de Toulouse, INPT, UPS, and CNRS, Allée Camille Soula, Toulouse F-31400, France*
[2]*Laboratoire de Génie Chimique (LGC), Université de Toulouse, INPT, UPS, and CNRS, 4 Allée Emile Monso, BP74233, Toulouse Cedex 4 F-31432, France*

We report an investigation of the wake of a sphere immersed in a uniform turbulent flow for sphere Reynolds numbers ranging from 100 to 1000. An original experimental setup has been designed to generate a uniform flow convecting an isotropic turbulence. At variance with previous works, the integral length scale of the turbulence is of the same order as the sphere diameter and the turbulence intensity is large. In consequence, the most intense turbulent eddies are capable of influencing the flow in the close vicinity of the sphere. Except in the attached region downstream of the sphere where the perturbation of the mean velocity is larger than the standard deviation of the incident turbulence, the flow is controlled by the incident turbulence. The distortion of the turbulence while the flow goes round the sphere leads to an increase in the longitudinal fluctuation and a decrease in the transversal one. The attenuation of the transversal fluctuations is still significant at 30 radii downstream of the sphere whereas the longitudinal fluctuations relax more rapidly toward the incident value. The more striking result however concerns the evolution of the mean velocity defect with the distance x from the sphere. It decays as x^{-2} and scales with the standard deviation of the incident turbulence instead of scaling with the mean incident velocity.

I. INTRODUCTION

The wake of a sphere set fixed in a uniform stationary flow is a classical well-documented problem of fluid mechanics, which depends only on the Reynolds number $\mathrm{Re}_S = U_\infty d / \nu$ based on the diameter d of the sphere, the velocity U_∞ of the incident flow, and kinematic viscosity ν of the fluid. When the Reynolds number increases, a wake experiences various regimes with dynamics of increasing complexity. The transitions between those regimes have been clearly identified[1,2] as well as the corresponding flow structure. In particular, the decay of the velocity defect with the distance x to the sphere evolves as x^{-1} in the laminar case[3] and as $x^{-2/3}$ in the turbulent one.[4,5]

The case of a sphere set fixed in a uniform turbulent incident flow is more complex since two different sources of fluctuations are present. In addition to wake instabilities that are mainly controlled by the Reynolds number Re_S (from now U_∞ will refer to the average incident velocity), the incident turbulence indeed makes another source of fluctuations. The elementary case of an incident turbulence that is fully developed and isotropic is characterized by three parameters: the standard deviation u'_∞ of any component of the velocity fluctuations, the integral length scale of the turbulence Λ, and the Taylor microscale λ. Several mechanisms then control the flow dynamics. In the vicinity of the sphere, the incident turbulence is distorted as it goes around the sphere. In return, the wake dynamics, flow separation, onset and development of instabilities, are influenced by the external turbulence. Farther downstream, the wake expansion depends on the turbulence within the wake, which results of both

wake instabilities and external turbulence that penetrates into the wake. On the other hand, external turbulence around the wake comes from incident turbulence distorted by the mean flow disturbance induced by the sphere. This two-way coupling mainly depends on the ratios of intensity, $I_t = \sqrt{3} u'_\infty / U_\infty$, and of length scales, Λ / d, between the incident turbulence and the wake.

As far as we know, three studies have been specifically devoted to this problem. Wu and Faeth[6,7] carried out an experimental investigation of the wake of a sphere for a large range of Reynolds numbers, for relatively large turbulence length scales and for rather low turbulence intensities (Table I). Legendre *et al.*[8] performed a large scale simulation for the same range of parameters ($\mathrm{Re}_S = 200$, $I_t = 0.04$, $\Lambda / d = 8$) and obtained results in agreement with those of Wu and Faeth. Bagchi and Balachandar[9] performed various direct numerical simulations in the same range of Reynolds numbers but for higher turbulence intensity ($I_t > 0.1$) and large turbulent length scales ($\Lambda / d > 53$).

All these works have been motivated by the goal of understanding the turbulence dynamics in dispersed two-phase flows, where the wakes of the particles play a major role. However, in high-Reynolds number bubbly flows,[10–12] intense turbulent eddies have a size comparable to that of the bubbles. The present work is thus an experimental investigation of the modification of the wake of a sphere by an isotropic incident turbulence that has simultaneously a large intensity and an integral length scale of the same order as the sphere diameter. We are interested to explore the range of Reynolds numbers $100 \le \mathrm{Re}_S \le 1000$, wherein the wake of a

sphere in a laminar incident flow changes from steady axisymmetric to strongly unsteady with vortex shedding. The objective is to determine the law of decay of the wake and to shed light on the mechanisms of turbulence distortion for this unexplored regime.

II. EXPERIMENTAL SETUP AND CHARACTERIZATION OF THE INCIDENT TURBULENT FLOW

To reach our objective we needed to generate a turbulent flow with the four following properties: (i) a uniform average velocity corresponding to Reynolds numbers Re_S ranging from 100 to 1000, (ii) an isotropic turbulence that is homogeneous over several tens of sphere diameters, (iii) an integral length scale close to the sphere diameter, and (iv) a large turbulence intensity. One may think to set the sphere on the axis of a channel flow, as Wu and Faeth[6,7] did. Obtaining a developed turbulence in a channel of width L however requires a Reynolds number $\mathrm{Re}_c = U_\infty L/\nu$ of at least 10 000. Since the integral length scale Λ in a channel flow is around $L/3$, the sphere should not be smaller than around $L/10$ to satisfy condition (iii). As a consequence, the Reynolds number Re_S cannot be smaller than 1000. At best, the channel flow can therefore allow to satisfy simultaneously either conditions (i) and (ii) for sphere diameters far smaller than Λ or (ii) and (iii). Inserting a grid upstream of the sphere makes Λ proportional to the grid mesh M and so makes it independent of the channel width. In this case, condition (iii) requires M being close to d. However, since M is then the characteristic length scale of the turbulence decay with the distance to the grid, the turbulence can hardly remain homogeneous along the wake and condition (ii) will not be satisfied. Moreover, the turbulence intensity would remain low, usually less than 0.1.

The present solution consists in generating the turbulence upstream of the channel rather than inside it. The flow loop is schematized in Fig. 1. A pump (2) supplies the water from a large tank (1) to sixty jets (3) discharging into a top reservoir (4) where the water level is maintained constant since a part of the flow goes out by an overfall (5). The jets generate an intense turbulent agitation that is convected by the flow which falls by gravity via a convergent section (6) into a square channel of width $L=0.22$ m (7). A test sphere of diameter $d=2$ cm (8) can be set on the axis of the channel, 0.9 m downstream of the inlet section. It is fixed on a stainless steel screw of 2 mm diameter mounted in tension between the two walls to prevent vibrations. In the following, the origin of spatial coordinates coincides in any case with the sphere center, the sphere being actually present or

not. The flowrate through the channel is adjusted by means of a valve (9) and a magnetic flowmeter (10) while the total flow rate through the pump (2) and the series of jets (3) remains constant.

Two-component velocity measurements have been carried out by laser Doppler anemometry (LDA) using a Spectra Physics 2016 argon laser operated in dual-beam (488–514.5 nm), forward-scattered, frequency-shifted mode and a burst spectrum analyzer (Dantec 55N10). A beam expander yielded a measurement volume having a diameter of 80 μm and a length of 660 μm. The flow was seeded with particles of iriodim 111 that can be considered as passive tracers. LDA time series of 360 s were recorded for each measurement points and then processed to obtain the average velocity U and the standard deviations u' and v' of the vertical and horizontal velocity components.
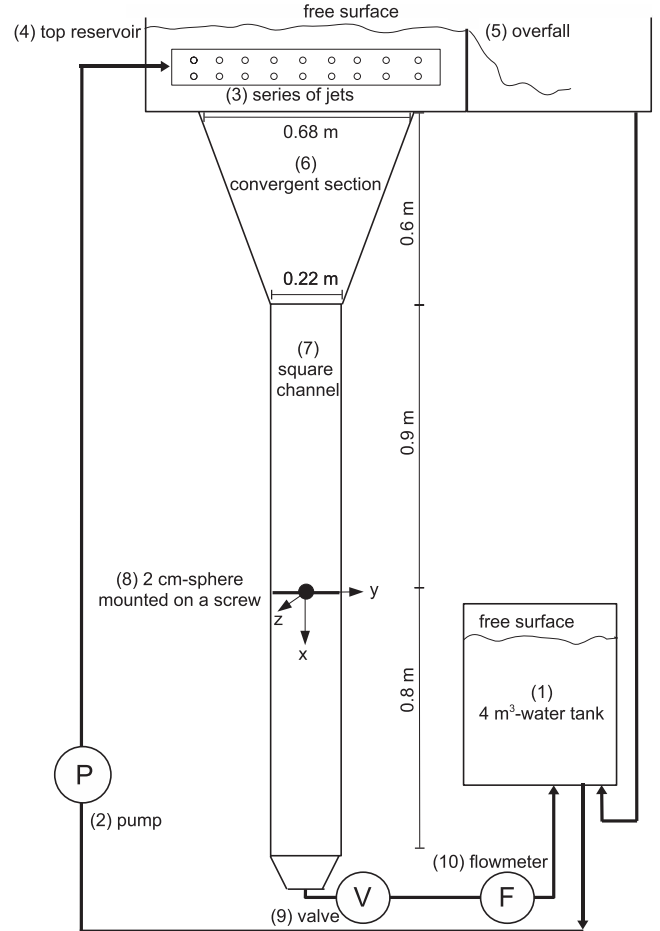

FIG. 1. Experimental setup.

TABLE II. Summary of present test conditions.

Case	U_∞ (cm/s)	$u'_\infty = v'_\infty$ (cm/s)	Re_S	I_t	Λ/d	Re_Λ	Re_λ	l_w/d
1	0.53	0.14	110	0.45	2.9	79	35	1.2
2	1.11	0.25	220	0.38	3.8	186	53	1.5
3	3.33	0.50	670	0.26	3.9	390	76	1.5
4	5.40	0.83	1080	0.26	2.9	479	85	1.5

In order to obtain channel Reynolds numbers Re_c ranging from 1000 to 12 000, we had to impose rather small incident velocities U_∞ ranging from 0.5 to 5.5 cm/s. The turbulent flow within the channel has been first characterized in the absence of the sphere and the turbulence properties of the four considered cases are listed in Table II. Figure 2(a) shows transverse profiles of average velocity U as well as the standard deviations u' and v' of the vertical and horizontal velocity components for three different Reynolds numbers. For case 1, due to the very small velocity ($U_\infty = 0.53$ cm/s), the data rate of the LDA system was only 10 Hz and it was difficult to ensure the convergence of the statistics. As a consequence, the accuracy on the determination of average velocity and standard deviations was not good: ± 0.05 cm/s, which corresponds to 10% of U_∞. That is the reason for the scatter of the results of case 1 in Fig. 2(a). For the other cases, since both the flow velocity is larger and the data rate rises up to 30 Hz, the accuracy on U, u', and v' is better than $\pm 2.5\%$ of U_∞ and the corresponding profiles show negligible scatter.

In any case, the flow is found to be homogeneous in the range $-6 \leq 2y/d \leq 6$. Moreover, u' and v' are equal, which indicates that the turbulence is isotropic. The magnitude of the fluctuations increases from 1.4 to 8.3 mm/s as the bulk velocity U_∞ increases from 0.53 to 5.4 cm/s (Table II). Due to the particular way for producing the turbulence upstream of the channel, the turbulence intensity differs between the different cases: $I_t = 0.45$ for case 1 and 0.38 for case 2 while

it is 0.26 for cases 3 and 4. On the other hand, the integral scale Λ remains almost constant ($2.9d - 3.9d$). Since the turbulence production is not related to the mean channel velocity, Re_c is not relevant to characterize the turbulence and will not be considered any longer. We thus introduce the Reynolds number based on the integral scale $\mathrm{Re}_\Lambda = u'_\infty \Lambda / \nu$ and the classic $\mathrm{Re}_\lambda = u'_\infty \lambda / \nu$ based on the Taylor microscale to characterize the turbulence.

Figure 2(b) presents the vertical evolution along the channel axis of the average U and the standard deviation u' of the vertical velocity for three different Reynolds numbers. Note that these quantities have been averaged over the transverse region $-6 \leq 2y/d \leq 6$ wherein the flow is homogeneous, which allows to obtain an accuracy for case 1 as good as for the other cases. One may notice a slight increase in the average velocity due to the development of the boundary layers at the channel walls and a small decrease in the fluctuation as the measurement point moves away from the region of production of the turbulence. These longitudinal evolutions are remarkably weak and we can consider that the flow is homogeneous regarding the wake development in the region extending from 30 radii above the sphere location to 30 radii below. However, when normalizing mean and fluctuating velocities within the wake, the properties of the channel flow at the corresponding axial location will be used in order to account for this slight inhomogeneity.

The spectral density of energy of the velocity fluctuations is determined from single-point measurements of the vertical velocity. The spatial spectra $PSDu'$ (which has been used to determine the integral lengthscale Λ) are then obtained by using the Taylor hypothesis. The spectra of all cases are presented in Fig. 3 as functions of the wavenumber k. They all show a classic $-5/3$ power-law range and, provided they are normalized by the corresponding variance and integral scale, appear to be the same over the range of k considered, although Re_λ varies from 35 to 85.

To sum up, the present set-up generates an isotropic turbulence, homogeneous over a region sufficiently large to
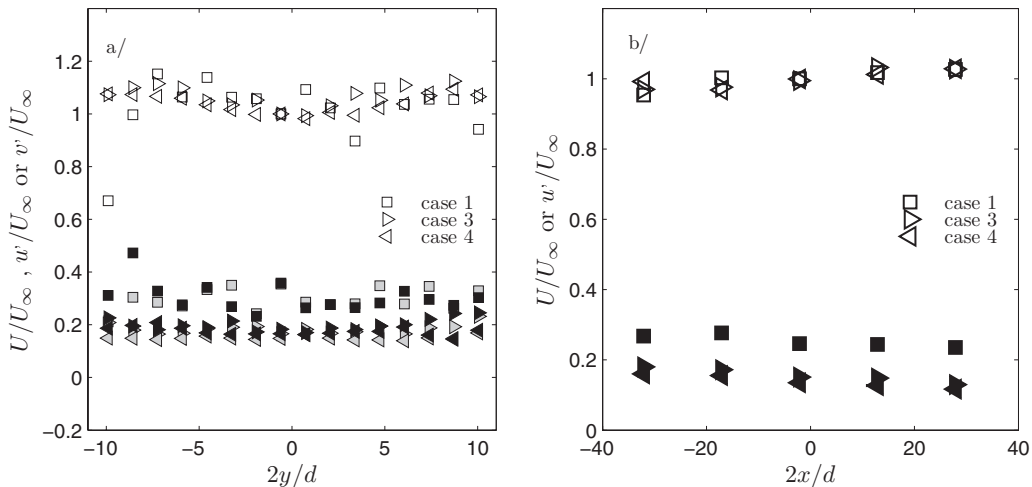

FIG. 2. Flow in the absence of the sphere. (a) Horizontal evolution in the channel midplane ($x=0$). (b) Vertical evolution of the flow on the channel axis. Empty symbols represent the mean velocity U, black symbols the standard deviation of the longitudinal velocity u', and gray symbols that of the transversal velocity v'. They are normalized by the mean velocity U_∞ at the origin of coordinates, which coincides with the sphere center. ($\square$) Case 1 ($\mathrm{Re}_S = 110$, $I_t = 0.45$, $\mathrm{Re}_\lambda = 35$). ($\triangleright$) Case 3 ($\mathrm{Re}_S = 670$, $I_t = 0.26$, $\mathrm{Re}_\lambda = 76$). ($\triangleleft$) Case 4 ($\mathrm{Re}_S = 1080$, $I_t = 0.26$, $\mathrm{Re}_\lambda = 85$).

FIG. 3. Spectra of the longitudinal velocity of the incident turbulence. ($\square$) Case 1 ($Re_S=110$, $I_t=0.45$, $Re_\lambda=35$). ($\bigcirc$) Case 2 ($Re_S=220$, $I_t=0.38$, $Re_\lambda=53$). ($\triangleright$) Case 3 ($Re_S=670$, $I_t=0.26$, $Re_\lambda=76$). ($\triangleleft$) Case 4 ($Re_S=1080$, $I_t=0.26$, $Re_\lambda=85$).
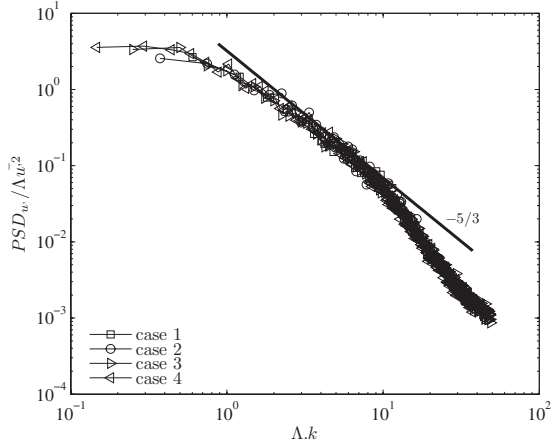
study the evolution of the sphere wake, with a relative intensity I_t larger than 0.2 and an integral length scale between $2.9d$ and $3.9d$. This properties are obtained for bulk velocities corresponding to sphere Reynolds numbers Re_S ranging from 100 to 1000.

III. RESULTS AND DISCUSSION

A. Mean velocity

We consider now the flow in the presence of the sphere. It is worth mentioning that the LDA data rate and the statistical convergence are better for the measurements performed in the region where the flow disturbance generated by the sphere is strong. As a consequence, the accuracy of case 1 is as good as the others cases from the sphere up to 3 radii downstream for points located within ± 6 radii about the axis, and up to 30 radii downstream for points located on the wake axis. In the following, we restricted the measurements of case 1 to this region. Therefore, the accuracy of all presented results is within $\pm 2.5\%$ of U_∞.

Figure 4 shows the evolution along the vertical axis of the sphere of the mean streamwise velocity U normalized by the incident average velocity U_∞. Upstream of the sphere, the mean flow starts decelerating around $2x/d=-5$ and vanishes on the sphere wall at $2x/d=-1$. The ratio U/U_∞ is in agreement with the potential flow prediction (represented by the line in the figure) and is therefore independent of Re_S as well as of the properties of the incident turbulence.

In the near wake ($1 \leq 2x/d \leq 2.5$), U is negative, which indicates the existence of a mean recirculating region. Defining the longitudinal extend l_w of this attached recirculating wake as the distance between the sphere rear and the location where U cancels again, we obtain $2l_w=1.2d$ for case 1 ($Re_S=110$, $I_t=0.45$) and $2l_w=1.5d$ for the others case ($Re_S \geq 220$, $I_t \leq 0.38$). The lengthening of the recirculating wake for increasing Re_S is a common observation.[13] However, l_w is shorter here than in the case of a laminar incident flow. Such a reducing effect of the incident turbulence on the length of the recirculating region was already noticed by
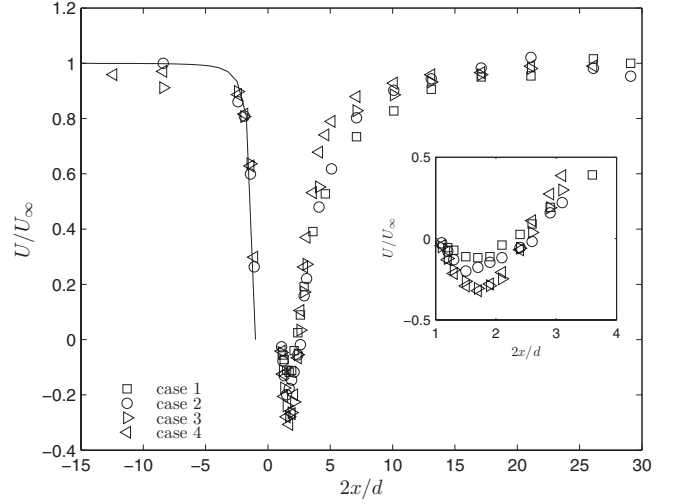
Bagchi and Balachandar,[9] but it is stronger in the present turbulent condition. Here, between case 1 and the others, the reduction in the turbulence intensity and the increase in Re_S work together to increase l_w. However, the main point is the remarkable matching of the profiles corresponding to $Re_S=670$ and 1080 (see the inset in Fig. 4), which suggests that at such a given turbulence intensity ($I_t=0.26$) the effect of the Re_S saturates.

Figure 5 shows the transverse profiles at $2x/d=2$ of the mean velocity defect $u_d=(U-U_\infty)$ and the transverse mean
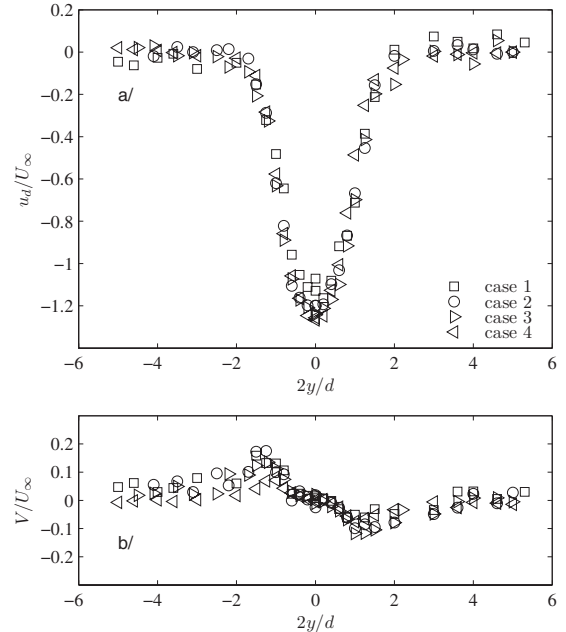

FIG. 4. Mean streamwise velocity along the vertical axis of the sphere. ($\square$) Case 1 ($Re_S=110$, $I_t=0.45$, $Re_\lambda=35$). ($\bigcirc$) Case 2 ($Re_S=220$, $I_t=0.38$, $Re_\lambda=53$). ($\triangleright$) Case 3 ($Re_S=670$, $I_t=0.26$, $Re_\lambda=76$). ($\triangleleft$) Case 4 ($Re_S=1080$, $I_t=0.26$, $Re_\lambda=85$). Continuous line: prediction for potential flow around a sphere.

FIG. 5. Transverse profiles of the streamwise U (a) and transverse V (b) mean velocities in the near wake at $2x/d=2$. ($\square$) Case 1 ($Re_S=110$, $I_t=0.45$, $Re_\lambda=35$). ($\bigcirc$) Case 2 ($Re_S=220$, $I_t=0.38$, $Re_\lambda=53$). ($\triangleright$) Case 3 ($Re_S=670$, $I_t=0.26$, $Re_\lambda=76$). ($\triangleleft$) Case 4 ($Re_S=1080$, $I_t=0.26$, $Re_\lambda=85$).
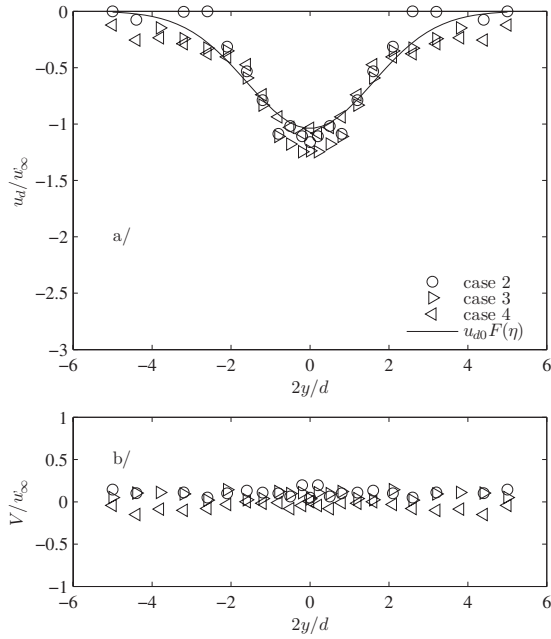
FIG. 6. Transverse profiles of the streamwise U (a) and transverse V (b) mean velocities at $2x/d=6$. ($\bigcirc$) Case 2 ($\mathrm{Re}_S=220$, $I_t=0.38$, $\mathrm{Re}_\lambda=53$). ($\triangleright$) Case 3 ($\mathrm{Re}_S=670$, $I_t=0.26$, $\mathrm{Re}_\lambda=76$). ($\triangleleft$) Case 4 ($\mathrm{Re}_S=1080$, $I_t=0.26$, $\mathrm{Re}_\lambda=85$). Continuous line: $u_d(x,y)=u_{d0}(x)\exp(-\eta^2/2)$ for case 4.

FIG. 7. Axial evolution of the mean velocity defect normalized by u'_∞ or U_∞. ($\square$) Case 1 ($\mathrm{Re}_S=110$, $I_t=0.45$, $\mathrm{Re}_\lambda=35$). ($\bigcirc$) Case 2 ($\mathrm{Re}_S=220$, $I_t=0.38$, $\mathrm{Re}_\lambda=53$). ($\triangleright$) Case 3 ($\mathrm{Re}_S=670$, $I_t=0.26$, $\mathrm{Re}_\lambda=76$). ($\triangleleft$) Case 4 ($\mathrm{Re}_S=1080$, $I_t=0.26$, $\mathrm{Re}_\lambda=85$).

velocity V normalized by the mean incident velocity U_∞. It confirms that the mean flow in the vicinity of the wake starts to be independent of the Reynolds number for $\mathrm{Re}_S>230$. In the transverse direction, the semiwidth of the wake, $l(x)$, is defined as the radial coordinate of the point where the velocity defect $u_d(x,y)$ is equal to $\exp(-1/2)$ times the value on the axis. It is approximately equal to $0.4d$ at $2x/d=2$ and does not depend on the considered case.

Figure 6 shows the transverse profiles at $2x/d=6$ of u_d and V normalized by the turbulence u'_∞: the velocity defect is already strongly attenuated, the mean transverse velocity is negligible, and the width of the wake is $l\approx0.8d$ for all cases. In agreement with Refs. 6–9 a classical self-similar law holds for the mean velocity defect: $u_d(x,y)=u_{d0}(x)F(\eta)$ with $u_{d0}=u_d(x,0)$, $\eta=y/l(x)$, and $F(\eta)=\exp(-\eta^2/2)$. However, the rate of expansion of the wake observed here, $dl/dx \approx0.2$, is much higher than in the study of Legendre et al.[8] who considered a similar length scale ratio Λ/d but a much lower turbulence intensity ($I_t=3.71\%$). Above all, it is remarkable that the velocity defects of all cases match well when normalized by the incident turbulence instead of the mean incident velocity.

Figure 7, which shows the mean velocity defect on the axis $u_{d0}(x)$, confirms for all cases the existence of two regions successively controlled by the mean and the fluctuating incident velocities. In the inset, the normalization by U_∞ shows the predominant role of the mean incident velocity in the near wake, up to 3 radii downstream of the sphere. Further downstream, the mean velocity defect scales as the intensity of the incident turbulence u'_∞ and decays as x^{-2}. All previous studies[6–9] have found decays as x^{-1} for $2x/d<30$. Nevertheless, Wu and Faeth,[6,7] as well as Legendre et al.,[8] have found that the decay was enhanced far from the sphere
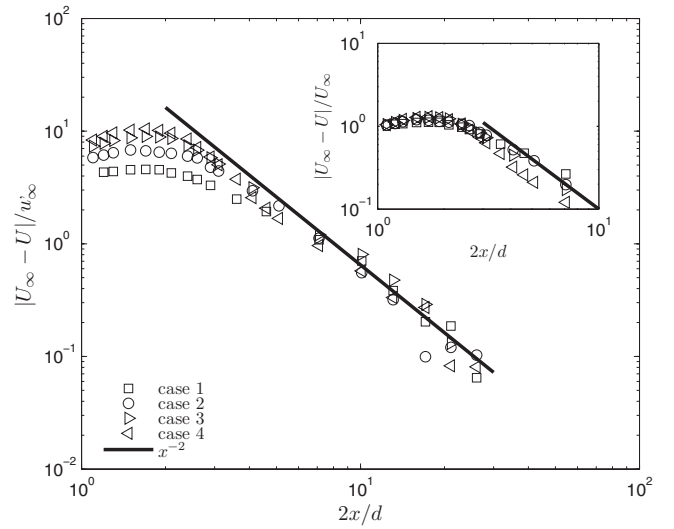
and followed a x^{-2} power law from the point where the intensity of the incident turbulence became greater than the mean velocity defect. In the present case, the incident turbulence seems thus intense enough to impose the x^{-2} law from $2x/d=5$, where $u'_\infty=0.5u_{d0}(x)$. However, the overall turbulence intensity is not sufficient to characterize the transition since its present value is similar to that of Bagchi and Balachandar.[9] The major difference between both cases is that the integral length scale of the incident turbulence is here of same order of magnitude as the diameter of the sphere, while in the study of Bagchi and Balachandar, it was nearly two orders of magnitude greater. The occurrence of the x^{-2} decay thus requires that the velocity fluctuations at the scale of the wake exceed the mean velocity defect. We have now to consider the evolution of the fluctuations downstream of the sphere.

B. Turbulence modulation

The evolution of the standard deviations of the longitudinal and transverse velocity fluctuations normalized by incident turbulence, u'/u'_∞ and v'/u'_∞, are plotted in Fig. 8 as a function of the longitudinal position along the axis. The longitudinal evolution of the mean flow has shown the existence of three different regions: upstream of the sphere the flow is potential, within the attached wake the mean velocity is dominated by the mean incident velocity and farther downstream it is controlled by the incident turbulence. The evolution of the fluctuations follows the same trends.

1. Upstream of the sphere

Let us consider first the region located upstream of the sphere. At $2x/d\approx-10$, the intensities of the fluctuations are close to their values in the absence of the sphere (see inset in Fig. 8). Just above the sphere ($-3<2x/d<-1$), the incident turbulence is however radically modified: u' is strongly attenuated whereas v' is significantly increased. Because the
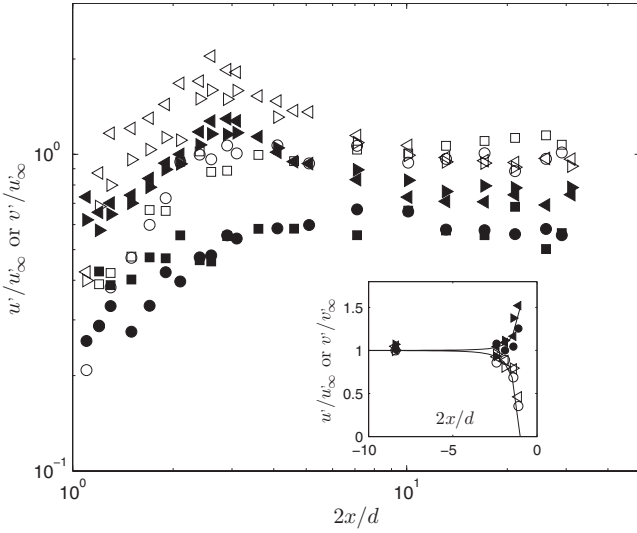
FIG. 8. Evolution along the axis of the fluctuations normalized by u'_∞. Empty symbols represent the standard deviation of the longitudinal velocity u', black symbols that of the transversal velocity v'. ($\square$) Case 1 (Re_S =110, I_t=0.45, Re_λ=35). ($\bigcirc$) Case 2 (Re_S=220, I_t=0.38, Re_λ=53). ($\triangleright$) Case 3 (Re_S=670, I_t=0.26, Re_λ=76). ($\triangleleft$) Case 4 (Re_S=1080, I_t =0.26, Re_λ=85). Continuous lines : RDT prediction by Durbin (u'/u'_∞ =$[1-(2x/d)^{-3}]$ and v'/v'_∞=$[1+0.5(2x/d)^{-3}]$).

turn-over time of the most energetic turbulent eddies (Λ/u'_∞) is large compared to the time required for a vortex to cross the sphere (d/U_∞), the phenomenon can be described by the rapid distortion theory (Britter *et al.*,[14] Durbin)[15] and results primarily from the distortion of the turbulent vorticity by the mean flow around the sphere and the blocking effect caused by turbulence impinging the sphere wall. Since the turbulent integral length scale is larger than the sphere ($\Lambda/d \approx 3-4$), the blocking effect is predominant and explains both the increase in v' and the attenuation of u' over a distance of order Λ. This interpretation is confirmed by the rather good agreement with the Durbin prediction, which is represented by the curves in the figure.

2. Attached wake ($1 \leq 2x/d \leq 3$)

We focus now on the region located immediately behind the sphere. On the axis, Fig. 8 shows that u' and v' increase monotically with the distance x to the sphere.

The evolution out of this axis shows a clear distinction between the agitation within the wake and the external turbulence. This is clearly visible in Fig. 9, where the transversal profiles at $2x/d=2$ of the fluctuations as well as those of the cross correlation have been normalized by either the mean incident velocity or the incident turbulence: on the left side are shown u'/U_∞, v'/U_∞, and $\overline{u'v'}/U_\infty^2$ while on the right side are plotted u'/u'_∞, v'/u'_∞, and $\overline{u'v'}/u_\infty'^2$.

In the central region ($2|y|/d \leq 2$) where there exists a significant mean velocity defect, the fluctuations are driven by the mean velocity U_∞: the vertical fluctuation u' dominates over the horizontal one and $\overline{u'v'}$ show maxima at the points where the gradient of U is maximum ($2|y|=2l=0.8d$). For cases 2-3-4, u'/U_∞ and $\overline{u'v'}/U_\infty^2$ are observed to depend only very slightly on both Re_S or I_t. For case 1, u' does not reach a maximum but rather increases
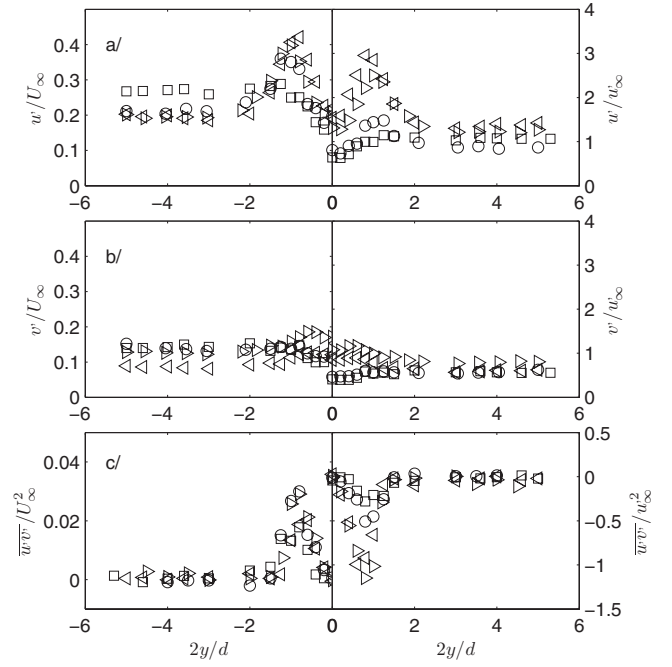

FIG. 9. Transverse profiles of the fluctuations at $2x/d=2$ normalized on the left hand side by the mean incident velocity U_∞ and on the right hand side by u'_∞. (a) Standard deviation of the longitudinal velocity u', (b) standard deviation of the transversal velocity v', and (c) shear stress $\overline{u'v'}$. ($\square$) Case 1 (Re_S=110, I_t=0.45, Re_λ=35). ($\bigcirc$) Case 2 (Re_S=220, I_t=0.38, Re_λ =53). ($\triangleright$) Case 3 (Re_S=670, I_t=0.26, Re_λ=76). ($\triangleleft$) Case 4 (Re_S =1080, I_t=0.26, Re_λ=85).

from a minimum located on the axis up to the incident value u'_∞ near $2|y|=d$. In the central region, velocity fluctuations thus scale with U_∞ and are weakly influenced by the intensity of the incident turbulence. This means that external perturbations do not penetrate into the recirculating wake and that the initial evolution of the velocity fluctuations on the axis results from the instability of the mean velocity profile. A complementary description of this phenomenon is obtained by analyzing the spectra of cases 2-3-4, which differ by their values of Re_S and Re_λ but have almost the same values of I_t and Λ/d. Figure 10 shows the longitudinal and transversal time spectra, $PSD_{u'}$ and $PSD_{v'}$, measured on the wake centerline. The measuring point is located at $2x/d=2.8$, where u' reaches its maximum for these cases. Two different frequency ranges have to be distinguished. At low frequencies ($\omega \leq U_\infty/d$), spectra are radically different from those of the incident turbulence and show similar trends for all cases, with a longitudinal component larger than that of the transversal one. Since the values of Re_S are moderate, a wide continuous spectrum of fluctuations cannot be produced by the instability of the near wake. However, no peak is present on the spectra indicating that the vorticity that is generated on the sphere is not periodically shed in the wake. This indicates that intense incident turbulence is capable to hinder periodic vortex shedding as observed by Ref. 9 for comparable I_t but much larger Λ/d. Fluctuations in the central region are thus probably generated by global wake oscillations and vortex emission that scale with U_∞ but are triggered by the random incident turbulence. At large frequency ($\omega \geq U_\infty/d$), case 2 is similar to the incident turbulence
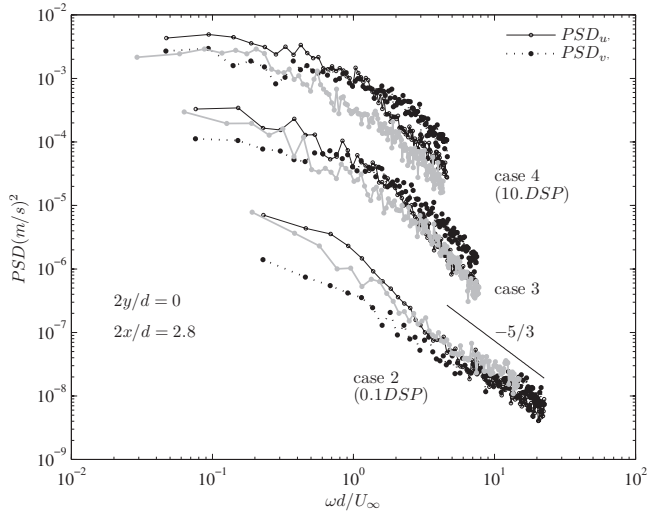
FIG. 10. Spectra of longitudinal and transversal fluctuations, PSD_u and PSD_v, at $2x/d=2.8$. (Gray line: spectrum in the absence of the sphere). The power spectral densities of longitudinal and transversal fluctuations, $PSD_{u'}$ and $PSD_{v'}$, have been determined by discrete Fourier transform of regularly resampled LDA times series and plotted as functions of $\omega=2\pi f$. The spectra corresponding, respectively, to case 2 and case 4 have been multiplied by 10 and 0.1 for sake of clarity. Case 2 ($Re_S=220$, $I_t=0.38$, $Re_\lambda=53$). Case 3 ($Re_S=670$, $I_t=0.26$, $Re_\lambda=76$). Case 4 ($Re_S=1080$, $I_t=0.26$, $Re_\lambda=85$).

FIG. 11. Transverse profiles of the fluctuations normalized by the incident turbulent velocity u'_∞ at $2x/d=6$. (a) Standard deviation of the longitudinal velocity u', (b) standard deviation of the transversal velocity v', and (c) shear stress $\overline{u'v'}$. ($\bigcirc$) Case 2 ($Re_S=220$, $I_t=0.38$, $Re_\lambda=53$). ($\triangleright$) Case 3 ($Re_S=670$, $I_t=0.26$, $Re_\lambda=76$). ($\triangleleft$) Case 4 ($Re_S=1080$, $I_t=0.26$, $Re_\lambda=85$).

whereas cases 3 and 4 are still radically different and show now a predominance of the transversal component.

Outside of the wake ($2|y|/d>2$), the fluctuations are driven by the turbulence coming from upstream. The right half of Fig. 9 shows that they are however different from the incident turbulence which has been distorted by passing the sphere. In all cases, even if the cross-correlation $\overline{u'v'}$ is negligible, the longitudinal component is dominant ($v'<u'$) and the transversal component is reduced ($0.5<v'/v'_\infty<0.8$). Concerning the longitudinal fluctuation, differences are observed between the cases: u' is almost the same as u'_∞ in case 1 whereas it is lower in case 2 and larger in cases 3 and 4. As mentioned before, the rapid distortion theory applied by Ref. 15 to a large-scale turbulent flow past a sphere predicts that u' is reduced while v' is increased at the upstream stagnation point. Just beside the sphere equator, the theory however predicts the reverse: u' is enhanced while v' is attenuated ($u'/u'_\infty=3/2$ and $v'/v'_\infty=0$ at the sphere wall). Due to the existence of the wake, it is not valid downstream of the sphere. We can however assume that the existence of the attached flow region prevents the turbulence from being distorted in a reverse way as it is convected from the equator to the region downstream of the sphere. That could qualitatively explain why $v'<u'$ out of the attached wake at $2x/d=2$, but cannot allow us to understand the precise role of the flow parameters and the differences observed between the four cases.

3. Open wake ($3\leq2x/d\leq30$)

Let us come back to Fig. 8 and consider the fluctuations in the open wake that develops beyond $2x/d=3$, which is approximately the location where the fluctuations attained their maximum in all cases. It is interesting to note that the
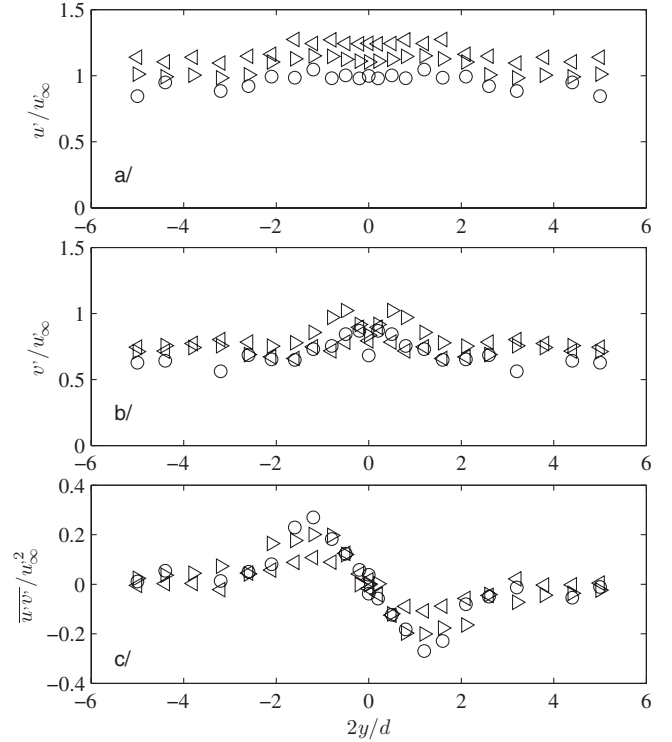
maxima of u'/u'_∞ observed here are similar to that measured by Wu and Faeth[6] for similar Re_S and Λ/d but lower I_t, while the present maximum of v'/u'_∞ is much smaller. In case 1, u' has already reached the value of the incident turbulence at $2x/d=3$ and no longer evolves with x, while v' has also attained a plateau but its value is still only close to $0.6v'_\infty$. In cases 2-3-4, u' is also larger than v' over all the investigated region and both components keep almost constant values from $2x/d\approx6$: u' has already reached the value of the incident turbulence ($u'/u'_\infty\approx1$) while v' is still significantly lower ($v'/v'_\infty\approx0.6$ for case 2 and $v'/v'_\infty\approx0.7-0.8$ for cases 3-4).

Above all, it is worth noting that in the region ($2x/d\geq5$) where the mean velocity defect scales as $u'_\infty(x/d)^{-2}$, the intensity of fluctuations are almost constant, which suggests that the production of fluctuations within the wake is no more the dominant mechanism. This is confirmed in Fig. 11 by the tranversal profiles of u'/u'_∞, v'/u'_∞, and $\overline{u'v'}/u'^2_\infty$ at $2x/d=6$ for cases 2-3-4. The best matching of the results is there obtained by normalizing the results by u'_∞ within both the central and the external regions. Compared to $2x/d=2$ (Fig. 9), the wake is twice larger and now extends up to $2|y|/d=4$, the profiles of the fluctuations u' and v' are much flatter and the Reynolds stress $\overline{u'v'}$ is strongly attenuated. However, at this location where the fluctuations are yet evolving slightly on the axis, u' and v' are still dependent on the properties of the turbulence.
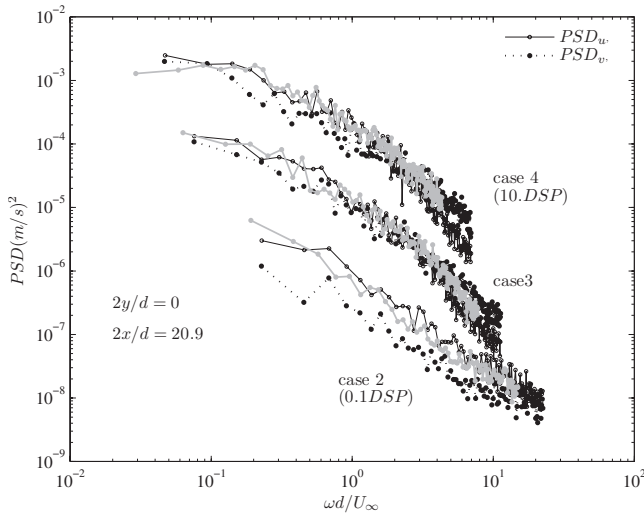
FIG. 12. Spectra of longitudinal and transversal fluctuations, PSD_u and PSD_v, at $2x/d=20.9$. (Gray line: spectrum in the absence of the sphere.) Note that since the results are close and exhibit the same trends, the spectra corresponding, respectively, to case 2 and case 4 have been multiplied by 10 and 0.1 for sake of clarity. Case 2 ($\mathrm{Re}_S=220$, $I_t=0.38$, $\mathrm{Re}_\lambda=53$). Case 3 ($\mathrm{Re}_S=670$, $I_t=0.26$, $\mathrm{Re}_\lambda=76$). Case 4 ($\mathrm{Re}_S=1080$, $I_t=0.26$, $\mathrm{Re}_\lambda=85$).

Figure 12 shows the time spectra of cases 2-3-4 at $2x/d=20.9$. For all the three cases, we observed that the relaxation of the vertical fluctuations to the incident turbulence is not restricted to the value of the variance but is achieved over the whole range of wavelengths. On the other hand, the lower intensity of the horizontal fluctuations appears to come from the attenuation of the large scales. The results of cases 3 and 4 are the same indicating that with similar turbulence intensity ($I_t=0.26$), the sphere and turbulent Reynolds numbers are large enough ($\mathrm{Re}_S=670$ and 1080, $\mathrm{Re}_\lambda=76$ and 85) to ensure that the results no more depends on them. The smallest scales are similar to those of the incident turbulence while the largest scales are attenuated. For case 2, which corresponds to a slightly larger turbulent intensity ($I_t=0.38$) but much lower Reynolds numbers ($\mathrm{Re}_S=230$, $\mathrm{Re}_\lambda=35$), the attenuation of the fluctuations is also affecting smaller scales. For all cases, the fluctuations result there from the distortion of the incident turbulence as it passes the sphere. Since $\Lambda=3-4d$, the region under consideration ($10\leq2x/d\leq30$) is located at less than 5Λ downstream of the sphere. It is therefore probably difficult for the largest turbulent eddies coming from upstream to join the axis after having circumvented the sphere. Let us now consider a turbulent vortex of radius R_w that has a horizontal axis. It generates both horizontal and vertical velocity fluctuations. However, it is only when the radial position of its center is less than $R_w/2$ that it can generate significant horizontal fluctuations within the wake. This may explain both why only horizontal fluctuations are attenuated within the wake and why this attenuation mostly concerns the large scales.

C. Conclusion: A wake controlled by the incident turbulence

We investigated the flow around a sphere set in a uniform turbulent incident flow with an integral length scale equal to about three sphere diameters and a turbulent intensity larger than 20%. Three regions have to be distinguished.

Upstream and besides the sphere the mean flow is almost potential and the incident turbulence is distorted in agreement with the prediction of rapid distortion theory.

Downstream of the sphere, an attached wake develops, the length of which ($1.2\leq l_w/d\leq1.5$) is shorter than in a laminar incident flow. Up to $2x/d=3$, the mean velocity and the intensity of the fluctuations within the wake scale with the mean incident velocity U_∞.

Around $2x/d=5$, the energy of the turbulent eddies whose size is close to that of the wake width becomes larger than the velocity defect. From that point, the wake appears to be controlled by the incident turbulence. First of all, the mean velocity defect of all considered cases is observed to collapse on a unique master curve and to scale with the intensity of the incident turbulence: $|U-U_\infty|=60(2x/d)^{-2}u'_\infty$. The attenuation of the wake is therefore faster in the present turbulent condition than for all regimes that have been previously investigated. Moreover, the turbulence is no more produced by the instability of the mean velocity profiles but results instead from the distortion of the incident turbulence by the sphere. Large energetic eddies are deviated from the wake axis by the presence of the sphere, which causes a lower level of horizontal fluctuations in the region located between 2Λ and 5Λ downstream of the sphere. Since, within the wake, both the turbulence is more intense than the velocity defect and the turbulent fluctuations are driven by the distorted incident turbulence, the evolution of the mean velocity defect is not the result of the continuous spreading of the initial perturbation of the mean-flow momentum by viscous and turbulent diffusions. The weak mean flow observed in this region is rather a consequence of the distortion of the strong incident turbulence. This is consistent with the fact that it scales with the incident turbulence. A theory of the turbulence distortion downstream of an obstacle accounting for the presence of an attached wake is however required to explain that it decays as x^{-2}.

[1]T. A. Johnson and V. C. Patel, "Flow past a sphere up to a Reynolds number of 300," J. Fluid Mech. **378**, 19 (1999).

[2]D. Ormières, and M. Provansal, "Transition to turbulence in the wake of a sphere," Phys. Rev. Lett. **83**, 80 (1999).

[3]G. K. Batchelor, *An Introduction to Fluid Dynamics* (Cambridge University Press, New York, 1967).

[4]H. Tennekes and J. L. Lumley, *A First Course in Turbulence* (The MIT Press, Cambridge, MA, 1972).

[5]M.S. Uberoi, and P. Freymuth, "Turbulent energy balance and spectra of axisymmetric wake," Phys. Fluids **13**, 2205 (1970).

[6]J. S. Wu, and G. M. Faeth, "Sphere wakes at moderate Reynolds numbers in a turbulent environment," AIAA J. **32**, 535 (1994).

[7]J. S. Wu and G. M. Faeth, "Effect of ambient turbulence intensity on sphere wakes at intermediate Reynolds numbers," AIAA J. **33**, 171 (1994).

[8]D. Legendre, A. Merle, and J. Magnaudet, "Wake of a spherical bubble or a solid sphere set fixed in a turbulent environment," Phys. Fluids **18**, 048102 (2006).

[9]P. Bagchi and S. Balachandar, "Response of the wake an isolated particle to an isotropic turbulent flow," J. Fluid Mech. **518**, 95 (2004).

[10]V. Roig and A. Larue de Tournemine, "Measurement of interstitial velocity of homogeneous bubble flows at low to moderate void fraction," J. Fluid Mech. **572**, 87 (2007).

[11]F. Risso, V. Roig, Z. Amoura, G. Riboux, and A. M. Billet, "Wake attenuation in large Reynolds number dispersed two-phase flows," Phil. Trans. R. Soc. London, Ser. A **366**, 2177 (2008).

[12]G. Riboux, F. Risso, and D. Legendre, "Experimental characterization of the agitation generated by bubbles rising at high Reynolds number," J. Fluid Mech. **643**, 509 (2010).

[13]R. Clift, J. R. Grace, and M. E. Weber, *Bubbles, Drops and Particles* (Academic, New York, 1978).

[14]R. E. Britter, J. C. R. Hunt, and J. C. Mumford, "The distortion of turbulence by a circular cylinder," J. Fluid Mech. **92**, 269 (1979).

[15]P. A. Durbin, "Distorted turbulence in axisymmetric flow," Q. J. Mech. Appl. Math. **34**, 489 (1981).